Optimization of the size ratio of Sn sphere and laser focal spot for an extreme ultraviolet light source

S. Yuspeh,[a] K. L. Sequoia, Y. Tao, M. S. Tillack, R. Burdt, and F. Najmabadi
Department of Electrical and Computer Engineering and the Center for Energy Research, University of California, San Diego, 9500 Gilman Drive, La Jolla, CA 92093-0438, USA

(Received 27 September 2008; accepted 6 November 2008; published online 3 December 2008)

The effect of the ratio of Sn sphere diameter to laser focal spot size (SD/FSS) on conversion efficiency (CE) from laser to in-band (2%) 13.5 nm extreme ultraviolet (EUV) light was investigated by fixing the laser spot size and irradiating variable diameter spheres. It was found that a minimum SD/FSS, i.e., 2.5, is necessary to produce high in-band CE, which is 15% higher than planar targets. Two-dimensional plasma density profile maps showed that the density of the dominant in-band EUV emission region and the size of the surrounding absorbing plasma can be manipulated by geometric effects of the SD/FSS ratio. © *2008 American Institute of Physics*. [DOI: 10.1063/1.3036956]

As the feature sizes of semiconductor microchips are becoming smaller, 193 nm optical lithography (ArF laser) is reaching its physical limitations for minimum node size. Extreme ultraviolet lithography (EUVL) is being developed as the next generation lithography technology for high volume manufacturing (HVM) for features 32 nm and below.[1] A lack of an affordable EUV source with long lifetime, high power, and high efficiency is preventing the commercialization of EUVL systems. Laser produced plasma has shown promise for the EUV light source used in HVM. Increasing the conversion efficiency (CE) from laser to in-band (2% bandwidth) EUV light will reduce the cost of ownership of the EUVL system. The reflective optics used in the EUVL system, i.e., multilayer Mo/Si mirrors, limit the wavelength of the EUV light used in EUVL to be 13.5 nm. There has been research focused on how laser intensity, spot size, pulse length, and target composition affects CE, but very little has been conducted on the ratio of the target to laser focal spot size.[2,3]

Experiments have shown that a planar target has higher CE than spheres[4] and vice versa.[5] In an EUVL system used for HVM, a liquid Sn droplet generator may be employed to produce spherical targets at 10 kHz. It is crucial to achieve the same high CE obtained with planar targets using small droplet targets. It has been shown that for a Sn plasma, the density profile plays a key role in the generation and transport of EUV light due to reabsorption of the EUV light induced by the plasma itself. Optimization of the plasma density profile is an effective way to control reabsorption of the EUV light and to enhance the in-band CE. For spherical targets, the ratio of sphere diameter to laser full width at half maximum (FWHM) focal spot size (SD/FSS) should be a key geometric factor in the evolution of the plasma. However, to date, there has been no experimental effort conducted to optimize the CE by varying target diameters.

In this report, we investigated the effect of the SD/FSS ratio on CE. In our experiments, glass spheres (with diameters from 80 to 330 μm) with approximately 2–3 μm of 99.999% pure Sn are employed as targets. The target is irradiated with a 1.064 μm neodymium doped yttrium aluminum garnet laser with a pulse length of 8 ns FWHM and 250 mJ of energy (so-called pump beam). The pump laser is focused to a 80 μm FWHM spot size. An absolutely calibrated EUV energy monitor (E-Mon) (from Jenoptik) is positioned at 39° from target normal, and a transmission grating spectrometer is positioned at 45°. The electron density of the plasma creates phase shifts in a probe beam as the probe beam passes through the plasma perpendicular to the pump beam. These phase shifts are seen using a Nomarski interferometer. Further experimental details can be found elsewhere.[6]

A time integrated EUV imaging system is used to view the in-band EUV emissions similar to that of Tao *et al.*[7] A Zr filter is placed between the plasma and a multilayer dielectric concave Mo/Si mirror which is perpendicular to the pump beam. The in-band EUV image is relayed onto an x-ray charge coupled device (CCD) camera at an angle of 25° with respect to the plane of laser incidence. The entire optical path is shielded to eliminate the effects of scattered light within the chamber. The image is recorded by a back-illuminated x-ray CCD camera (Princeton Instruments Pi-SX). The system has a 5× magnification with spatial resolution better than 5 μm.

The measured in-band CEs of Sn spherical targets with different SD/FSS ratios integrated over a 2π solid angle are shown in Fig. 1. The angular distribution measured by Sequoia *et al.* under the identical conditions with the present

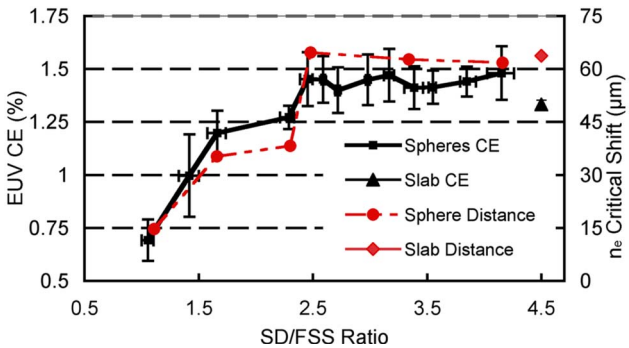

FIG. 1. (Color online) The in-band EUV CE in a 2π sr for spheres of 80–330 μm corresponding to a 1.1–4.3 SD/FSS ratio (black squares) and the critical density plasma shift along the laser axis (red circle). Also plotted is the planar target CE (black triangle) and critical density shift (red diamond).

[a]Electronic mail: syuspeh@ucsd.edu.

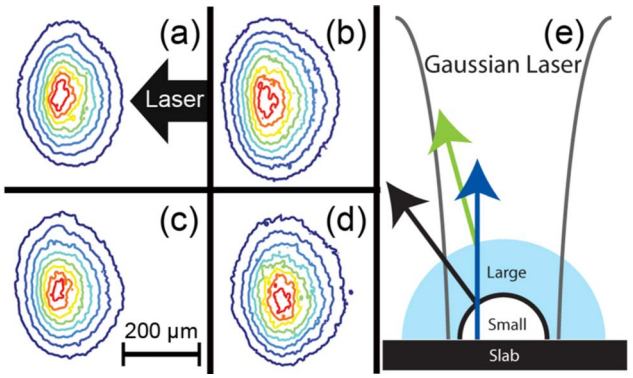

FIG. 2. (Color online) Normalized time integrated EUV emission image for (a) 1.35, (b) 3.53, (c) 3.99 SD/FSS ratio, and (d) planar targets. (e) Direction of plasma expansion for a small, large, and slab target from a single spatial location of the laser.

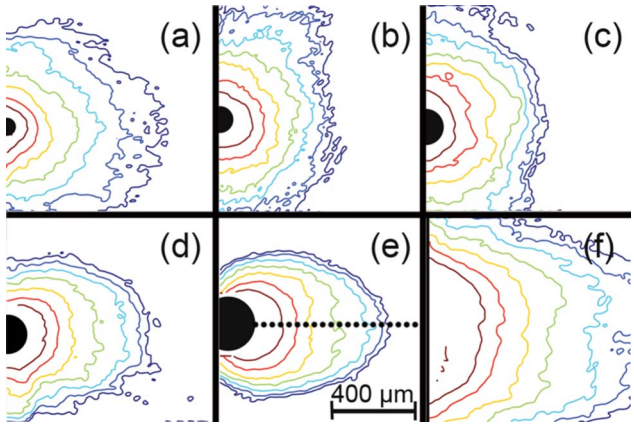

FIG. 3. (Color online) log 10 of the plasma density at the peak of the laser pulse for SD/FSS ratios of (a) 1.11, (b) 1.66, (c) 2.30, (d) 2.48, (e) 3.34, and (f) planar. The contour lines correspond to log 10 values of 17.5–19 in 0.25 increments.

experiments is used to calculate the in-band CE.[8] The collected data are binned every 0.125 SD/FSS ratio, and at least four samples are in each bin. The large error bars are caused by fluctuations in the laser and small alignment errors (<5 μm). It is seen in Fig. 1 that there are four distinct regimes in the data; a linear regime (below 1.6 SD/FSS ratio), a flat regime (1.6–2.25 SD/FSS ratio), a gain regime (2.25–2.5 SD/FSS ratio), and a saturation regime (above 2.5 SD/FSS ratio). Previously, researchers have used targets with size comparable to that of the spot size (approximately equivalent to our 2.0 SD/FSS ratio), which does not yield the highest CE.[4,9,10] By increasing the size of the target beyond a 2.5 SD/FSS ratio, one can improve the CE by 20%, which would also be 15% higher than planar targets.

The in-band EUV images of Sn plasma of spheres with diameters of 108, 283, and 315 μm and a planar plate were recorded, and typical results are shown in Figs. 2(a)–2(d), respectively. It is seen in Figs. 2(a)–2(d) that the shape of the in-band EUV emission and the distance from the target surface were relatively consistent for all size spheres and the planar target. The in-band EUV emission peak is located at approximately 180 μm in front of the target with lateral FWHM width approximately equal to $1/e^2$ of the laser focal spot size. It reveals that any plasma outside this emission region has insignificant contributions to the in-band EUV emissions, and the emission region is independent of the plasma expansion and density. Therefore, the density of ions in the in-band emission region directly impacts the amount of in-band EUV being generated.

The plasma density maps of Sn spheres with SD/FSS ratios of 1.11, 1.66, 2.30, 2.48, 3.34, and planar target observed at the peak of the 8 ns pump laser pulse are shown in Figs. 3(a)–3(f), respectively. The mathematical algorithm to transform the interferograms to density profile maps can be found elsewhere.[2,11] The distance from the target surface to the critical surface along the laser axis [dotted line in Fig. 3(e)] follows the same trend as the CE and is plotted for comparison in Fig. 1. The critical surface area expands longitudinally to 14.7, 35.3, 38.2, 64.7, 62.7, and 63.7 μm for SD/FSS ratios of 1.11, 1.66, 2.30, 2.48, 3.34, and planar, respectively. The critical surface shifts toward the laser, creating higher density in the dominant in-band EUV emission region shown in Fig. 4. The increased plasma density in the dominant in-band emission region generates more in-band EUV due to higher ion density. The CE depends on the quantity of in-band EUV being generated by the dominant in-band emission region and the amount of in-band EUV being reabsorbed by the surrounding plasma. Whereas the critical surface shift corresponds to the density in the dominant emission region and therefore the amount of in-band EUV light being generated, the plasma scale length relates to the amount of in-band EUV light being reabsorbed by the surrounding plasma. The plasma scale length is a fitted exponential decay function $\exp(-x/l_s)$ of the plasma density along the laser axis where l_s is the plasma scale length. A larger scale length means that there are more ions for the generated in-band EUV light to travel past, increasing the reabsorption of EUV light. The planar target's plasma scale length along the line of laser incidence is larger, 165 μm compared to 135 μm for spheres in the saturation regime (Fig. 4), yielding a larger reabsorption layer affecting the spectral emissions and hydrodynamic energy.

Figure 2(e) shows a simple sketch of the direction of the plasma expansion from a single spatial location of the pump laser for a small sphere, a large sphere, and a slab target. Smaller spheres produce more lateral expansion because the plasma expands normal to the target surface.[12] The impact of the lateral expansion varies depending on the SD/FSS ratio. The plasma is only heated while in the path of the laser beam; therefore any plasma that expands beyond the beam during the laser pulse is no longer heated by the laser and begins to cool, eventually reaching temperatures not suitable

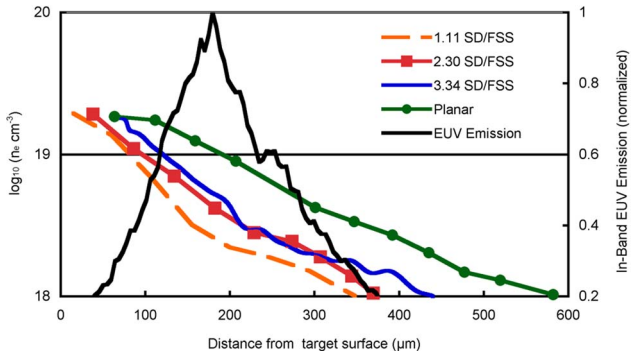

FIG. 4. (Color online) Typical plasma densities along the laser axis for SD/FSS ratios of 1.11 (orange dash), 2.30 (red square), 3.34 (blue), and planar target (green circle). Also plotted is the time integrated in-band EUV emission along the laser axis (black).

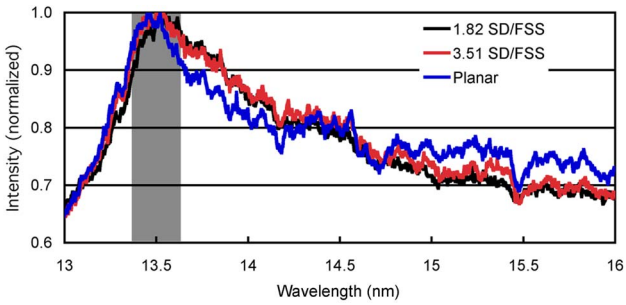

FIG. 5. (Color online) Typical soft x-ray spectra at 45° for SD/FSS ratios of 1.82, 3.51, and planar with the in-band EUV region shaded.

for efficient in-band 13.5 nm EUV generation. Illustrated as the small sphere in Fig. 2(e), the lateral expansion is wasting energy by transferring laser energy from inside the beam path to outside the beam path and also impacts the generation of in-band EUV in the dominant emission region by reducing the ion density. The CE in the linear regime steadily increases because the laser beam is larger than the diameter of the target, so the percentage of the laser energy incident on the target, the mass ablation, and the density of ions in the in-band emission region all increase as the target diameter increases. In the flat regime, the majority of the energy is already incident on the targets, and the sphere sizes have little impact on the plasma expansion [Figs. 3(b) and 3(c)], creating a fairly flat CE.

However, the plasma lateral expansion decreases throughout the gain regime until most of the plasma is contained within the beam path, as shown as the large sphere in Fig. 2(e). This causes a large jump in the CE in the gain regime and a dramatic change in the density profile [Figs. 3(c) and 3(d)]. Once the plasma is contained within the laser path, there is no longer significant wasted energy in lateral expansion. Throughout the saturation regime, the geometric effect of the sphere diameter has little impact on the plasma expansion, and the CE remains constant. With planar targets, the increase in plasma density begins to have the opposite effect on CE. The size and opacity of the absorbing plasma surrounding the in-band EUV emission region increases to the point where the higher density increase the absorption of the in-band EUV more than the generation of in-band EUV. Planar targets produce an overdense plasma for this application, creating a larger scale length leading to more in-band EUV reabsorption by the plasma itself. The higher intensity portion of the Gaussian laser beam continually interacts with the same electrons throughout the entire laser pulse in planar targets due to the reduction of lateral expansion, thus increasing the plasma scale length. This does not occur with the sphere in the saturation regime due to electrons having a small amount of lateral expansion.

The effects of the absorption layer of the plasma can be seen by typical normalized soft x-ray spectra for 1.82 and 3.51 SD/FSS ratios and a planar target shown in Fig. 5. The normalized spectra for all sphere sizes showed no substantial differences due to the fact that the plasma is underdense. Therefore, there is no significant dependence on the absorption of the in-band EUV and the sphere diameter. However, the planar target shows a shift in the in-band emission region at around 13.5 nm caused by opacity and size of the plasma.[13] The dominant in-band emission region is approximately 280 μm long, obtained from the EUV imaging, and is surrounded by an absorptive plasma layer. The larger plasma scale length of planar targets means that there is an increase in absorption of the in-band EUV.

It has been shown that a minimum SD/FSS ratio is required to produce the highest possible CE for spherical Sn targets at prototypical commercial EUVL system parameters. Three factors, i.e., mass ablation, lateral expansion, and reabsorption of EUV light, play key roles in the plasma evolution and in-band CE for Sn spheres. For very small spheres, the laser beam overfills the target reducing the mass ablation. The plasma also expands laterally beyond the laser beam with small spheres in which a large portion of the mass being ablated is not heated to temperature required for in-band EUV generation. This does not only waste energy but also reduces the density of the plasma in the dominant in-band EUV emission region. A large jump in CE is obtained when the SD/FSS ratio is large enough so that the plasma expansion mainly remains in the path of the laser beam and there is still some lateral expansion creating a smaller absorption layer than that of planar targets. The planar target plasma is too dense, having a large absorption layer while having the same size in-band emission region. The ideal conditions at these parameters are SD/FSS ratios beyond 2.5, which is higher than what is currently used. So, the opacity and size of the plasma can be changed using different diameter spheres generating an optimum SD/FSS ratio for high in-band CE.

This work was supported by Cymer Inc. and by the University of California (UC) under the UC Industry-University Cooperative Research Program (ele06-10278).

[1]P. J. Silverman, J. Microlithogr., Microfabr., Microsyst. **4**, 011006 (2005).
[2]Y. Tao, S. S. Harilal, M. S. Tillack, K. L. Sequoia, B. O'Shay, and F. Najmabadi, Opt. Lett. **31**, 2492 (2006).
[3]T. Okuno, S. Fujioka, H. Nishimura, Y. Tao, K. Nagai, Q. Gu, N. Ueda, T. Ando, K. Nishihara, T. Norimatsu, N. Miyanaga, Y. Izawa, and K. Mima, Appl. Phys. Lett. **88**, 161501 (2006).
[4]M. S. Tillack, K. L. Sequoia, and Y. Tao, J. Phys.: Conf. Ser. **112**, 042060 (2008).
[5]A. Sunahara, A. Sasaki, and K. Nishihara, J. Phys.: Conf. Ser. **112**, 042048 (2008).
[6]Y. Tao, M. S. Tillack, S. S. Harilal, K. L. Sequoia, and F. Najmabadi, J. Appl. Phys. **101**, 023305 (2007).
[7]Y. Tao, H. Nishimura, T. Okuno, S. Fujioka, N. Ueda, M. Nakai, K. Nagai, T. Norimatsu, N. Miyanaga, K. Nishihara, and Y. Izawa, Appl. Phys. Lett. **87**, 241502 (2005).
[8]K. L. Sequoia, Y. Tao, S. Yuspeh, R. Burdt, and M. S. Tillack, Appl. Phys. Lett. **92**, 221505 (2008).
[9]N. Nishimura, S. Fujioka, T. Okuno, Y. Tao, N. Ueda, T. Ando, T. Aota, Y. Yasuda, S. Uchida, Y. Shimada, M. Yamaura, J. Hashimoto, Q. Gu, K. Nagai, Y. Norimatsu, H. Furukawa, Y. G. Kang, A. Sunahara, K. Gamada, M. Murakami, K. Nishihara, M. Miyanaga, Y. Izawa, and K. Mima, J. Phys. IV **133**, 1189 (2006).
[10]S. George, C. S. Koay, K. Takenoshita, R. Bernath, M. Al-Rabban, C. Keyser, V. Bakshi, H. Scott, and M. Richardson, Proc. SPIE **5751**, 779 (2005).
[11]L. B. Da Silva, T. W. Barbee, Jr., R. Cauble, P. Celliers, D. Ciarlo, S. Libby, R. A. London, D. Matthews, S. Mrowka, J. C. Moreno, D. Ress, J. E. Trebes, A. S. Wan, and F. Weber, Phys. Rev. Lett. **74**, 3991 (1995).
[12]L. Láska, J. Krása, M. Pfeifer, K. Rohlena, S. Gammino, L. Torrisi, L. Andò, and G. Ciavola, Rev. Sci. Instrum. **73**, 654 (2002).
[13]S. Fujioka, H. Nishimura, K. Nishihara, A. Sasaki, A. Sunahara, T. Okuno, N. Ueda, T. Ando, Y. Tao, Y. Shimada, K. Hashimoto, M. Yamaura, K. Shigemori, M. Nakai, K. Nagai, T. Norimatsu, T. Nishikawa, N. Miyanaga, Y. Izawa, and K. Mima, Phys. Rev. Lett. **95**, 235004 (2005).